

RSC Advances



This is an *Accepted Manuscript*, which has been through the Royal Society of Chemistry peer review process and has been accepted for publication.

Accepted Manuscripts are published online shortly after acceptance, before technical editing, formatting and proof reading. Using this free service, authors can make their results available to the community, in citable form, before we publish the edited article. This *Accepted Manuscript* will be replaced by the edited, formatted and paginated article as soon as this is available.

You can find more information about *Accepted Manuscripts* in the [Information for Authors](#).

Please note that technical editing may introduce minor changes to the text and/or graphics, which may alter content. The journal's standard [Terms & Conditions](#) and the [Ethical guidelines](#) still apply. In no event shall the Royal Society of Chemistry be held responsible for any errors or omissions in this *Accepted Manuscript* or any consequences arising from the use of any information it contains.

Poly(3,4-ethylenedioxythiophene)/MoS₂ nanocomposites with enhanced electrochemical capacitance performance

Jin Wang*^a, Zongchao Wu^a, Huabing Yin^b, Wei Li^a, Yang Jiang^c

^a School of Chemical engineering, Hefei University of Technology, Hefei 23009, China

^b Department of Electronics and Electrical Engineering, University of Glasgow, G12 8QQ, UK

^c School of Materials Science and Engineering, Hefei University of Technology, Hefei 23009, China

*Corresponding author. Tel.: +86 551 62905660; fax: +86 551 62905660.

E-mail address: jinwang@hfut.edu.cn (Jin Wang).

ABSTRACT: Composites based on conducting polymer and two-dimensional (2D) layer structure transition metal oxides are expected to realize the combination of good mechanical properties and excellent capacitance. Here poly (3, 4-ethylenedioxythiophene) / molybdenum disulfide (PEDOT/MoS₂) intercalated composites were successfully synthesized via *in-situ* polymerization in the presence of ammonium persulfate (APS). The thermal stability, conductivity and capacitance performance are improved significantly with increasing fraction of MoS₂. When the content of MoS₂ was 45 % in weight, the maximum weight loss velocity temperature is 365 °C which is 52 °C higher than that of PEDOT, the specific capacitance was 405 F/g about 4 times that of a PEDOT electrode, also capacity retention was around 90% after 1000 cycles. This study provides a facile preparation method of organic/inorganic nanocomposites with enhanced electrochemical capacitance performance.

Keywords: poly(3,4-ethylenedioxythiophene); molybdenum disulfide; intercalated composites; supercapacitor

1 Introduction

Supercapacitors possess outstanding properties such as the high power density typical of conventional capacitors together with the high energy density typical of rechargeable batteries. In addition, supercapacitors also exhibit fast charge-discharge processes and a long cycle life. These advantages mean they are expected to become an efficient and practical energy storage device¹. Research into supercapacitors is largely focused on improving performance, reducing cost and improving the environmental friendliness of the devices. The most commonly used electrode materials include carbon material², transition metal oxides³⁻⁴ and conductive polymers⁵⁻⁸. There are limitations to a single species used for electrodes active materials, like carbon nanotubes, graphene and its derivatives typically have lower specific capacitances than conductive polymers, ruthenium dioxide (RuO₂) can suffer from poisoning, and conductive polymers usually possess poor cycle stability. These factors limit their application as electrode materials in supercapacitors⁹⁻¹⁰. Composites of conductive polymers and inorganic materials offer a promising combination of cycle stability, cost-efficiency and good capacitance performance¹¹⁻¹².

Supercapacitors work based on two charge-storage mechanisms: surface ion adsorption (electric double layer capacitance) and redox reactions (pseudocapacitance)¹³. Conducting polymers are so-called pseudocapacitors, i.e., they store charge, not only in the electrical double layer, but also faradaically in the polymer matrix¹⁴. Among these conductive polymers, poly (3,4-ethylenedioxythiophene) (PEDOT) possess the potential to be used as an electrode due to its superior conductivity and stability¹⁵. Additionally, PEDOT has a larger electrochemical window compared to other conducting polymers. It has been reported that PEDOT can be composited with transition metal oxide, graphene and carbon materials to prepare electrode materials¹⁶⁻¹⁸. Two-dimensional (2D) layered compounds such as graphite and transition metal oxides can offer a large surface area to storage charge, resulting in good characteristics for electric double layer capacitance¹⁹⁻²⁰. Molybdenum disulfide (MoS₂) is a typical 2D layered material that is non-toxic, available at low cost and has been confirmed to have high specific capacity and cycle stability when used as an

anode material ²¹. The layered MoS₂ can be anticipated to exhibit good capacitive properties due to its sheetlike morphology, which provides a large surface area for double-layer charge storage. In addition, the transition metal Mo center can exhibit a range of oxidation states from +2 to +6, providing it pseudocapacitance abilities similar to RuO₂. Composites based on PEDOT and 2D layered MoS₂ are expected to offer the synergetic combination of good mechanical properties and excellent capacitance derived from both charge-storage mechanisms.

Conjugated polymer/MoS₂ composites can be prepared by means of the exfoliating / restacking technique of Li_xMoS₂. First, MoS₂ was intercalated by lithium to form Li_xMoS₂ and exfoliated into the single-molecule-layer MoS₂ suspension in water, and then in the process of MoS₂ restacked, polymers can be inserted into the layered host MoS₂ in the following two ways: (1) direct insertion approach, where the polymer are first dispersed in solvent and then inserted into the MoS₂ layered structure; (2) *in-situ* intercalation / polymerization approach, where the intercalated monomer was inserted first, followed the monomer polymerized in the present of MoS₂. As for the former, Polyaniline (PANI) and its intercalation compounds PANI/MoS₂ have been prepared by mixing a solution of PANI and a suspension of single-layer MoS₂ ²²⁻²³. However, the effect of mixing is dependant on the solubility of the conjugated polymer. For most conjugated polymers, poor solubility limits their application in composites. *In-situ* intercalation / polymerization are the facile approach for the fabrication of conjugated polymer/MoS₂ composites. The composites of MoS₂ and conjugated polymers such as polypyrrole, polythiophene and its derivates have been prepared by this method ²⁴⁻²⁶. The study on PEDOT/MoS₂ composites used for capacitor has not been reported.

The purpose of this work is to enhance the capacitance properties of PEDOT electrode materials via introduction of 2D layer MoS₂. PEDOT/MoS₂ intercalated composites were synthesized via *in-situ* polymerization in a single layer suspension of MoS₂ with APS as an oxidizing agent. The structure, thermal stability and capacitance performance were examined and the relationship between structure and properties are discussed. The well-defined intercalated structures of PEDOT/MoS₂ composites

exhibit improved thermal stabilities and capacitance properties. It can be deduced that a synergistic effect occurs between PEDOT and MoS₂ interlayer.

2 Experimental

2.1 Materials

EDOT monomer (99%), N-Butyllithium (1.6 M solution in hexane) was obtained from Aladdin industrial Inc. MoS₂ (99%) is from Hefei Kehua Fine Chemical Industry Research Institute. APS, methanol and acetone are from Sinopharm Chemical Reagent Co., Ltd.

2.2 Synthesis of PEDOT/MoS₂ nanocomposites

The suspension of single layer MoS₂ was prepared based on the literature²⁷. Commercial raw 2H-MoS₂ was soaked in 1.5 equivalents butyllithium and kept in a Nitrogen atmosphere for 3 days. The Li_xMoS₂ product was then exfoliated in water (~100mL) through a redox reaction. 0.8 mL EDOT was added into a three-necked flask with the different number of single layer MoS₂ suspension (10, 20, 30 mL). This solution was stirred until a homogeneous distribution was obtained. 3.42 g of APS (EDOT/APS molar ratio is 1:2) was dissolved into deionized water and added dropwise to the flask followed by mechanical stirring for 72 h at the room temperature. The reaction product was washed using a methanol/acetone mixture (methanol / acetone volume ratio is 2:1) followed by distilled water and then put into a vacuum drying oven for desiccation (24 h at 60 °C). The PEDOT/MoS₂ intercalated composites with 14 wt%, 30 wt% and 45 wt% contents of MoS₂ were named PEDOT/MoS₂-14, PEDOT/MoS₂-30, PEDOT/MoS₂-45, respectively. PEDOT without acid doping was also synthesized as above for comparison.

2.3 Characterization

X-ray diffraction (XRD) data were recorded using a Rigaku D/Max-2550 diffractometer with Cu-K α radiation ($\lambda=1.5418$ Å). The morphology of MoS₂ and PEDOT/MoS₂ nanocomposites was examined using a field emission scanning electron microscope (FE-SEM, SU8020, Hitachi, Japan, operated at an acceleration voltage of 5 kV and equipped with an energy-dispersive X-ray (EDX) spectrometer and a field emission transmission electron microscope (FE-TEM, JEM-2100F, JEOL,

Japan, operated at an accelerating voltage of 200 kV). The surface chemical properties of PEDOT/MoS₂ nanocomposites were investigated using EDX spectrometer. The thermal stabilities of all PEDOT/MoS₂ samples were characterized using a TG 209 F3 (Netzsch, Germany) with a heating rate of 10 °C/min under N₂ atmosphere. Electrical conductivity at room temperature was determined using a conventional four-probe method on pressed pellets, formed under a pressure of 20 MPa with a diameter of 10mm. Cyclic voltammetry (CV), constant current charge-discharge tests and electrochemical impedance spectroscopy (EIS) experiments were conducted using a CHI660B electrochemical workstation with a three-electrode system. The working electrode was prepared by mixing the PEDOT/MoS₂ powder, carbon black and polyvinylidene fluoride (PVDF) binder (85:10:5 by weight). The mixture (~ 0.007g) was pressed onto the steel mesh (~ 30mm²), and dried under vacuum for 3h at 60 °C. The thickness of the working electrode is about 0.3mm. We can think these values are constant. Blank platinum was used as the counter electrode. Ag/AgCl was used as the reference electrode. Experiments were carried out at ambient temperature using 1M H₂SO₄ aqueous solution as an electrolyte.

3. Results and discussion

3.1 Structure and morphology

The structures of PEDOT, restacked MoS₂ and PEDOT/MoS₂ composites were confirmed by FT-IR spectra. As shown in Fig.1, the presence of peaks at 1382 and 1350 cm⁻¹ (C–C and C=C stretching vibrations of thiophene ring), 1204 and 1095 cm⁻¹ (C–O–C stretching vibrations in ethylene oxide unit), 984 and 694 cm⁻¹ (C–S stretching vibrations in thiophene ring) prove the formation of PEDOT. The peak at about 465 cm⁻¹ in restacked MoS₂ is assigned to Mo-S stretching mode of vibration. In comparison with pure PEDOT, the presence of peak at about 465 cm⁻¹ in PEDOT/MoS₂ composites proves the existence of MoS₂. The intercalation of PEDOT into the MoS₂ host layers is demonstrated by powder X-ray diffraction. Fig.2 (a) provides the XRD pattern of the dry restacked MoS₂. This presents an obvious (002) diffraction peak, indicating that the MoS₂ layer is still regularly restacked along the c-axis. The restacked MoS₂ shows broadened peaks and a shortened (002) diffraction

peak, suggesting that the mean crystallite size of the restacked MoS₂ is much smaller than that of raw bulk 2H-MoS₂²⁸. The typical XRD patterns of PEDOT/MoS₂ composites are shown in Fig.2 (b). The (001) diffraction peak is observed with shifts to lower angles that indicates an increase in interlayer spacing. The middle strong (001) peak at 6.54 ° corresponds to $d = 13.79 \text{ \AA}$. Compared with bulk MoS₂, the interlayer spacing of MoS₂ in the intercalation composites was expanded by approximately 7.64 Å due to the intercalation of PEDOT. The strong c-axis peaks at $2\theta = 14.3^\circ$ (Fig.2b) also reveals that partial MoS₂ is still regularly restacked along the c-axis without sandwiching PEDOT, and partially intercalated PEDOT/MoS₂ composites are obtained in our experiment. The data from the PEDOT/MoS₂ composites also shows another two broad peaks at ca. $2\theta = 18^\circ$ and 26° which are different from those of MoS₂ and should attributed to the diffraction patterns of PEDOT²⁹, indicating the periodicity parallel and perpendicular characteristics of the polymer chain. Charge storage in MoS₂ can occur via intersheet or intrasheet double-layer charge storage modes²¹, and the well-ordered PEDOT/MoS₂ intercalation composites offer the potential of being good electrode materials.

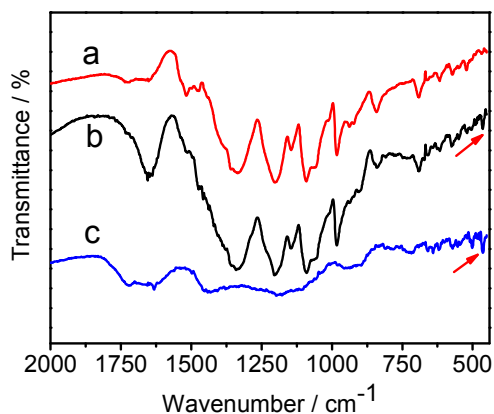


Fig.1 FT-IR spectra of PEDOT(a), PEDOT/MoS₂ composites (b) and restacked MoS₂ (c)

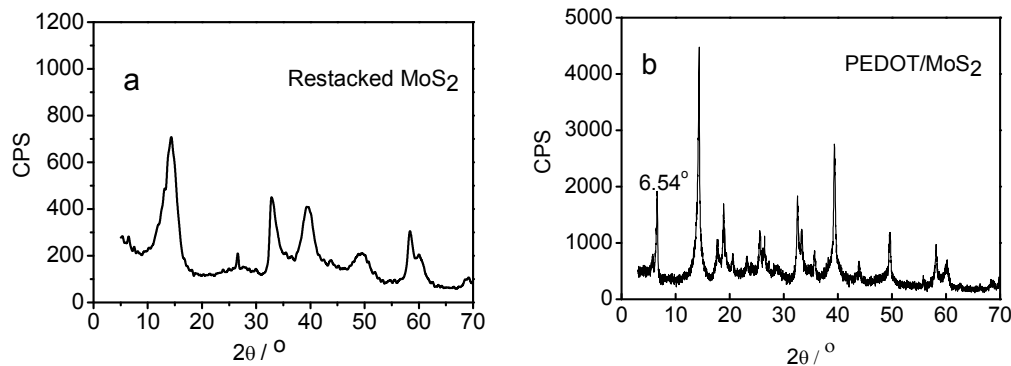


Fig.2 XRD patterns of restacked MoS₂ (a) and PEDOT/MoS₂ composites (b)

The morphology and the chemical surface characteristics of MoS₂ and PEDOT/MoS₂ composites were characterized by TEM, SEM and EDX. The TEM image of as-prepared exfoliated MoS₂ shows thin layered particles with a typical size of 350 nm long and 200 nm wide (Fig.3a). The 2D lamellar MoS₂ with higher specific surface area of MoS₂ is favorable for double layer capacitive properties in comparison with bulk MoS₂. These MoS₂ structures have exhibited typical single-crystal features, as revealed by the SAED pattern (inset in Fig.3c). The HRTEM image does show lattice fringes corresponding to MoS₂ (Fig.3b), two kinds of lattice spacing of 0.273 nm can be observed in the magnified HRTEM image, corresponding to the (100) and (101) planes of standard MoS₂, respectively (Fig.3c). The combinations of SEM and EDX methodologies not only help to observe PEDOT/MoS₂, they also provide information on the two-dimensional, physico-chemical nature of the composites. Scanning electron micrographs of PEDOT/MoS₂ composites are presented in Fig.3 (d, e) and EDX spectrograms are shown in Fig.3 (f). The morphology of the conjugated polymer strongly depends upon the nature of the anionic oxidizing agents used and preparation methods. As shown in Fig.3 (d), PEDOT/MoS₂ composites took on a uniform state with plate like structure, which is different from the nanoribbon like structure of PEDOT/MoS₂ composites produced using FeCl₃ as an oxidizing agent²⁶. The existence of Mo, S, C and O are evidenced from EDX analysis performed on the surface of the composites (Fig.3f), suggesting that MoS₂ and PEDOT exist in the composites. Furthermore, the elemental composition of PEDOT/MoS₂ can be calculated by EDX measurements, its chemical ratios of Mo, S, C and O are 35.4 wt%, 28.8 wt%,

30.5 wt% and 5.3 wt%, respectively, which is in general agreement with the product expected from the experiment, showing the composites are uniform.

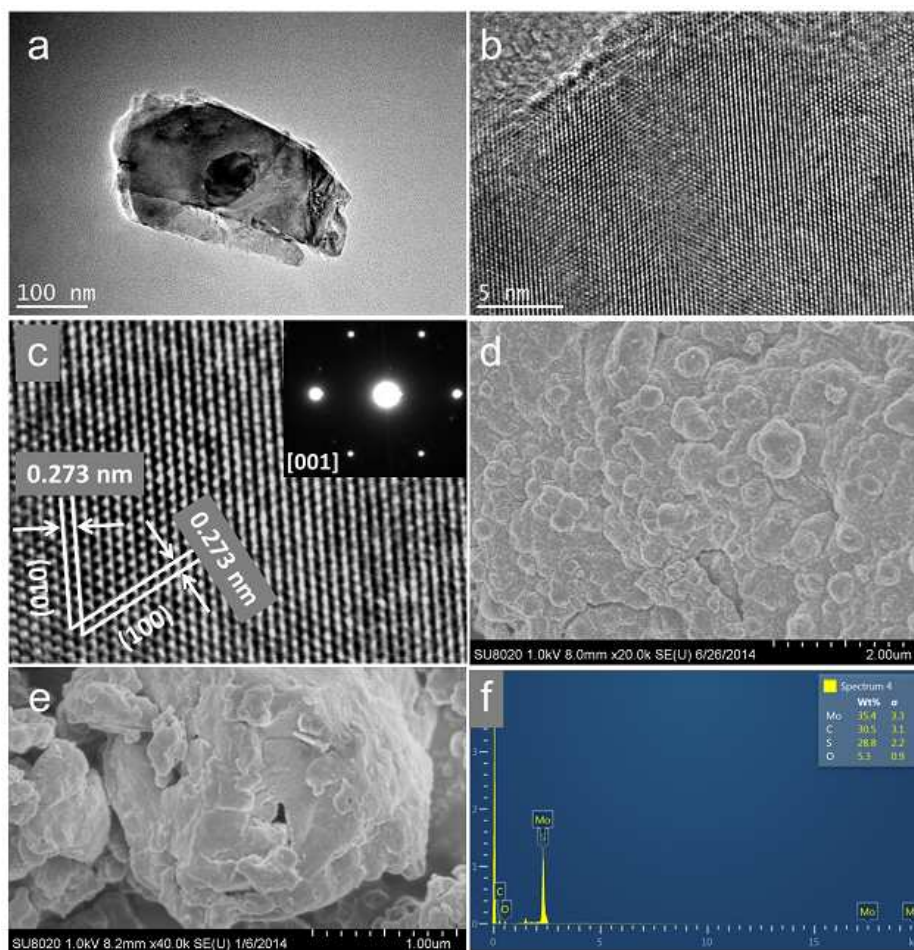


Fig.3 TEM and HR-TEM images of Li-intercalated MoS₂ (a, b, c), SEM of PEDOT/ MoS₂ (d, e), EDX pattern of PEDOT/MoS₂ (f)

3.2 Thermal analysis

The thermal analysis of PEDOT and PEDOT/MoS₂ nanocomposites in N₂ atmosphere was obtained using TGA experiments as shown in Fig.4. All the samples exhibited slight weight loss in the range of 100~150 °C, which can be ascribed to the loss of water. The mass loss which occurs between 250 °C and 400 °C could be attributed to the combustion and departure of the organic polymer components. The maximum weight loss velocity temperature of pure PEDOT and PEDOT/MoS₂ nanocomposites are seen at 313 °C, 323 °C, 349 °C and 365 °C, respectively. It is clear that the thermal stability of PEDOT/MoS₂ intercalated composites were better

than that of PEDOT, and the thermal stability of PEDOT/MoS₂ increased with increasing content of MoS₂. 2D layered nanomaterials can improve the properties of polymers, including strength, modulus, thermal stability and gas barrier effects³⁰. MoS₂ used as 2D layered nanofillers in PEDOT/MoS₂ composites increase the thermal stability of the PEDOT matrix due a physical barrier effect which retards the diffusion of degradation products, gases and heat. The mass loss is followed by a slight continuous weight loss up to 600 °C, which can be attributed to the complete departure of residual polymer components. There is still 31 % weight remaining in pure PEDOT when the temperate reaches 800 °C. This should be attributed to the carbonization of the conjugate ring structure of PEDOT at high temperatures. The remaining weight of PEDOT/MoS₂ composites are are around 41 %, 54 % and 62 % at 800 °C, respectively. The weight percentage of MoS₂ in PEDOT/MoS₂ intercalation composites can also be determined by TGA. The weight percentage of MoS₂ can be calculated in the following way. After heated to 800 °C, MoS₂ (weight percentage = x) and the residual of PEDOT (0.31(1-x)) remains. So we have $x+0.31(1-x) = 0.41, 0.54, \text{ and } 0.62$. The corresponding weight percentages of MoS₂ are 14 %, 30 % and 45 %, respectively.

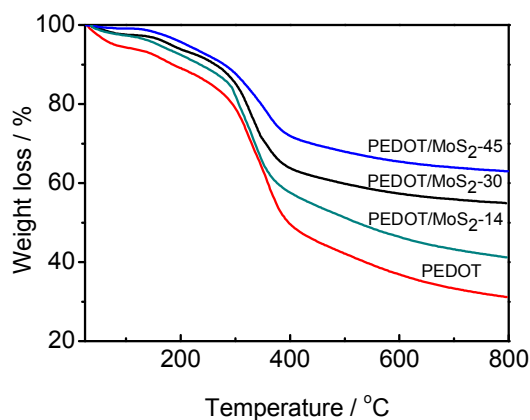


Fig.4 TGA curves of PEDOT and PEDOT/MoS₂ composites

3.3 Electrical Conductivity

Room temperature electrical conductivities were measured on pellets pressed from powders. The conductivity values of restacked MoS₂, pure PEDOT and PEDOT/MoS₂ nanocomposites are summarized in Table 1. The measured conductivity values of

restacked MoS₂ and PEDOT were $1.37 \times 10^{-2} \text{ S cm}^{-1}$ and $2.43 \times 10^{-2} \text{ S cm}^{-1}$, respectively. However, the measured conductivity values of PEDOT/MoS₂ nanocomposites without any acid doping are an order of magnitude higher than that of each component, i.e., restacked MoS₂ and pure PEDOT. These values increased with increasing amount of MoS₂. The electrical conductivity values of PEDOT/MoS₂-14, PEDOT/MoS₂-30, and PEDOT/MoS₂-45 are $5.56 \times 10^{-1} \text{ S cm}^{-1}$, $7.53 \times 10^{-1} \text{ S cm}^{-1}$ and $9.10 \times 10^{-1} \text{ S cm}^{-1}$, respectively. The increase of electrical conductivity in intercalated composites is explained by an interaction between conductive PEDOT and MoS₂ layers. The conducting macromolecules of PEDOT with conjugated π -bonds intercalated into the host interlayer of MoS₂ are arranged in a layered arrangement according to the XRD analysis as above. This architecture is advantageous for transportation of electrons between the organic and inorganic components. Moreover, intercalation of MoS₂ with Lithium results in a structural transformation from trigonal prismatic to octahedral metal coordination and a change in properties from semiconducting to metallic³¹. Increasing the contents of metallic restacked MoS₂ in PEDOT/MoS₂ nanocomposites can improve the conductivity property.

In comparison with FeCl₃ as oxidizing agent²⁶, PEDOT/MoS₂ produced using APS as oxidizing agent in this work showed higher conductivity. The electrical conductivity of composites is related to the particle size and shape³². Higher surface area for electron transfer is usually favorable for increasing electron mobility, and the smaller particle size provides a higher surface area for electron transfer. The particle size and shape of synthesized PEDOT depends on the oxidant type, PEDOT nanoparticles using APS as the oxidizing agent showed a smaller particle size and higher electrical conductivity than FeCl₃. The conductivity of the conjugated polymer is also related to the length of their conjugated chain. The addition of inorganic compounds may decrease the degree of conjugated π bonds in the polymer when using an improper synthesis method^{26, 33}. APS using as the oxidizing agent can provide a better stability polymerization system in comparison to using FeCl₃ as an oxidizing agent. The progressive conductivity of PEDOT/MoS₂ intercalation composites reported here indicates that the preparation method is a facile approach for

organic / inorganic composites.

Table 1 the data of electrical conductivities

sample	restacked MoS ₂	PEDOT	PEDOT/MoS ₂ -14	PEDOT/MoS ₂ -30	PEDOT/MoS ₂ -45
Conductivity (S cm ⁻¹)	1.37×10 ⁻²	2.43×10 ⁻²	5.56×10 ⁻¹	7.53×10 ⁻¹	9.10×10 ⁻¹

3.4 Electrochemical characteristics

The electrochemical behavior of the samples when used as active electrode materials was investigated using CV, EIS and constant current charge-discharge tests in 1.0 M H₂SO₄ aqueous solution. Fig.5 illustrates the CV performance of pure PEDOT and PEDOT/MoS₂ intercalation composites with different MoS₂ contents at a scan rate of 50 mV/s in the potential window range of -0.2~0.8 V. These data are normalized to the geometric area of the electrode surface. The voltammograms reveal high electrochemical reversibilities of PEDOT and PEDOT/MoS₂ intercalation composites at this potential range and sweep rate. In comparison to pure PEDOT, the CV curves PEDOT/MoS₂ intercalation composites show a deviation from the rectangular shape, whereby the CV profile resembles an ‘S’-shape, which suggesting the coexistence of charge storage mechanisms with double layer charge storage and pseudocapacitive faradic charging. The curves show no obvious peaks, indicating that the capacitor assembled using a PEDOT/MoS₂ nanocomposite electrode has fast charge and discharge properties³⁴. By comparison, the area of the CV curve for the PEDOT/MoS₂ nanocomposite is larger than those of the pure PEDOT electrode, indicating higher specific capacitance and the synergistic effect of PEDOT and MoS₂. In this case the charge carrier within the electrodes could be more effective and rapid due to the interaction between PEDOT and MoS₂ layers. Furthermore, the CV curve area increases at the same scan rate as the fraction of MoS₂ increases, indicating that the capacitance of PEDOT/MoS₂ nanocomposites increases with the increase in the MoS₂ content. The increase of specific capacitance also suggests that MoS₂ in the composites contributes greatly to the specific capacitance.

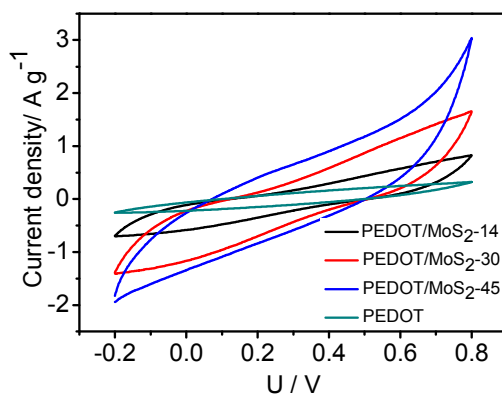


Fig.5 CV curves of pure PEDOT and PEDOT/ MoS₂ composites at scan rate of 50 mV/s

Electrochemical impedance measurements were used to study the redox processes of the PEDOT/MoS₂ nanocomposites and to evaluate their ionic and electronic conductivity as well as specific capacitance. The Nyquist plots for PEDOT and PEDOT/MoS₂ nanocomposites with different MoS₂ content are shown in Fig.6. Impedance was tested in the frequency range from 0.05 kHz to 100 kHz at open-circuit potential. The impedance value was composed of the resistance of the electrode, electrolyte and the contact resistance at the interface active material / current collector. There is great similarity in the Nyquist plots for all of these materials. At high frequency, the plots of PEDOT and PEDOT/MoS₂ intercalation composites all show favourable semicircles which is indicative of the charge transfer phenomena of a faradic redox process. The diameter of the semicircle corresponded to interface charge transfer resistance (R_{ct}). The R_{ct} of PEDOT/MoS₂ is smaller than that of PEDOT, showing PEDOT/MoS₂ composites have the faster charge transfer rates. Meanwhile, the R_{ct} of PEDOT/MoS₂ composites decreased with increasing fraction of MoS₂. This indicates that the addition of MoS₂ reduces charge transfer resistance and improves the conductivity of the electrode materials. At low frequency, the line is almost vertical to the real axis in the imaginary part of the impedance demonstrating an ideal capacitive behavior for PEDOT/MoS₂ nanocomposites. This ideal capacitive behavior is attributed to the faradic pseudo-capacitance of the composite electrodes³⁵. This conclusion agrees with the capacitance properties above.

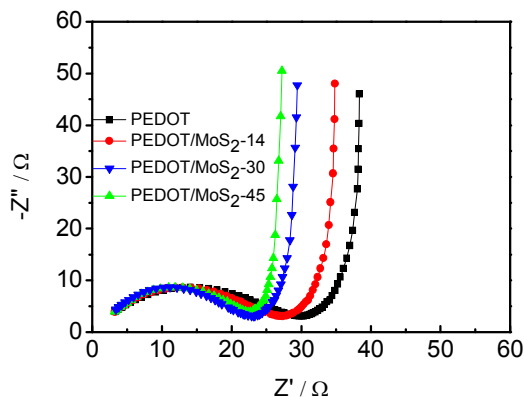


Fig.6 Nyquist impedance spectra of pure PEDOT and PEDOT/ MoS₂ composites

3.4 Charge-discharge cycling performance

The galvanostatic charge-discharge curves of PEDOT and PEDOT/MoS₂ are displayed in Fig.7 (a). It can be observed that all the charge-discharge curves of PEDOT and PEDOT/MoS₂ took on the shapes that closed to a triangle, and show distinct characteristics of reversible charge-discharge. Particularly, PEDOT/MoS₂ composites have longer charge / discharge times than PEDOT as can be ascribed to their high capacitance performances. The specific capacitance can be evaluated using the following equation³⁶:

$$C_g = \frac{I\Delta t}{\Delta V \times m} \quad (1),$$

Where C_g (F/g) is the specific capacitance of the electrode, I (A) is the discharge current, Δt (s) is the discharge time, ΔV (V) is the potential window and m (g) is the mass of active materials loaded in working electrode. According to the equation, the specific capacitance of PEDOT can be calculated as 109 F/g. The discharge time of PEDOT/MoS₂ composites increased with increasing MoS₂ content. The specific capacitances of PEDOT/MoS₂-14, PEDOT/MoS₂-30 and PEDOT/MoS₂-45 are 208 F/g, 354 F/g and 405 F/g, respectively. The specific capacitance of the PEDOT/MoS₂-45 sample reached four times that of pure PEDOT. This gives clear proof that a synergistic effect of PEDOT and MoS₂ allows a higher capacitance for the composite electrode which derived from both charge-storage mechanisms. Hang et al.³⁷ and Ma et al.³⁸ has reported the composites of PANI/MoS₂ and PPy/MoS₂ respectively, in which the preparation method of conducted polymer/MoS₂ composites

is mainly through chemical synthesis from Mo precursors such as sodium molybdate ($\text{Na}_2\text{MoO}_4 \cdot \text{H}_2\text{O}$). PANI/ MoS_2 composites exhibit a specific capacitance of 575 F/g at a current density of 1 A/g in a three-electrode system, which is about two times than that of pure PANI. The composites of PPy and MoS_2 afforded a high specific capacitance of 553.7 F/g at a current density of 1 A/g in a typical three-electrode test, which is also about two times than that of pure PPy. The specific capacitance of these composites all higher than each of the composition, and shows the synergistic effect in conducted polymer/ MoS_2 composites. For comparison, the preparation of PEDOT/ MoS_2 nanocomposites in this work shows a more effective improvement method in supercapacitance performance.

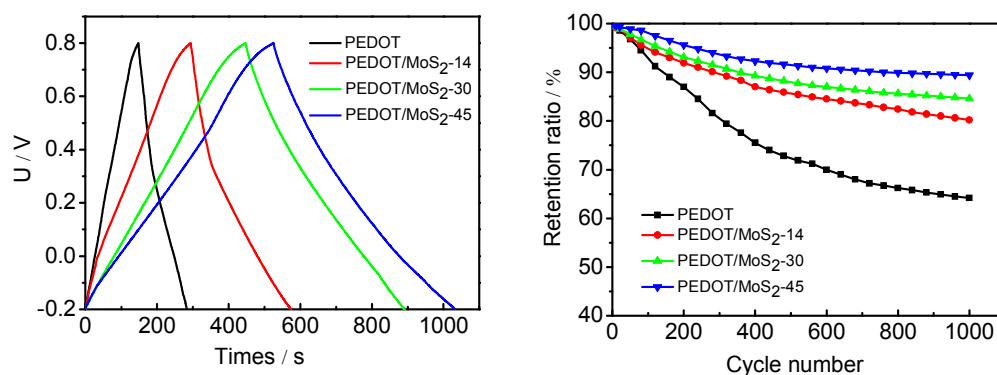


Fig.7 Galvanostatic charge-discharge curves (a) and cycle stability (b) of electrodes with pure PEDOT and PEDOT/ MoS_2 at current density of 0.8A/g

The cycling stability of PEDOT and PEDOT/ MoS_2 nanocomposite electrodes was measured by charge/discharge cycling at a current density of 0.8 A/g. As shown in Fig.7 (b), the specific capacitance of PEDOT is only 64 % after 1000 charge/discharge cycles, while the PEDOT/ MoS_2 nanocomposite electrodes displayed greater cycle stability, with this stability increasing with increasing fraction of MoS_2 . The specific capacitance of the PEDOT/ MoS_2 -45 sample decreased only 5 % after 200 cycles, holding steady at 90 % from 300 cycles to 1000 cycles. This demonstrates that PEDOT/ MoS_2 -45 has good long-term cycle stability. These studies suggest that the composite electrodes have fast charge exchange, leading to good cyclic power storage ability. The excellent cycling stability can be explained by the following two reasons: (1) the higher specific surface area of MoS_2 is favorable to the rapid diffusion

of ions by providing a low-resistance pathway and (2) the intercalation of conjugated polymer into the MoS₂ interlayer facilitates electron transport during the charging and discharging processes because of its high conductivity. This result is also in agreement with the thermal stability analysis above, i.e., the better thermal stability of PEDOT/MoS₂ brings smaller volume change during the charge/discharge processes.

4 Conclusions

A facile synthesis method of PEDOT/MoS₂ nanocomposites has been developed via *in-situ* polymerization in the presence of ammonium persulfate. The well-defined intercalated structure of PEDOT/MoS₂ nanocomposites is beneficial to their conductivity, thermal stability and capacitance. The conductivity, thermal stability and the specific capacitances of the PEDOT/MoS₂ nanocomposites were enhanced by increasing the amount of MoS₂, exhibiting a good synergetic effect between an inorganic layered compound and organic polymer. When the content of MoS₂ was 45 % in weight, the specific capacitance achieved was 405 F/g, about 4 times larger than that of a PEDOT electrode. The PEDOT/MoS₂ nanocomposite also retained a capacity of around 90% after 1000 cycles. This work offers a strategy for preparing supercapacitors with high performance and good stability.

Acknowledgements

This work was financially supported by National Natural Science Foundation of China (Grant No. 61076040), Anhui Provincial Natural Science Foundation (Grant No. 1208085MB23).

References

- [1] A. Burke, J. Power Sources, 2000, 91(1), 37.
- [2] S. L. Candelaria, Y. Y. Shao, W. Zhou, X. L. Li, J. Xiao, J. G. Zhang, Y. Wang, J. Liu, J. H. Li and G. Z. Cao, Nano Energy, 2012, 1, 195.
- [3] S. Chen, J. W. Zhu, X. D. Wu, Q. F. Han and X. Wang, Acs Nano, 2010, 4, 2822.
- [4] D. Choi, G. E. Bloragren and P. N. Kumm, Adv. Mater., 2006, 18, 1178.
- [5] K.Firoz Babu, S. P. Siva Subramanian and M. Anbu Kulandainathan, Carbonhydr. Polym., 2013, 94(1), 487.
- [6] S.R. P. Gnanakan., M. Rajasekhar and A. Subramania, Int. J. Electrochem. Sci., 2009, 4, 1289.
- [7] Q. Liu, O. Nayfeh, M. H. Nayfeh and S. T. Yau, Nano Energy, 2013, 2, 133.

- [8] J. F. Mike and J. L. Lutkenhaus, *J. Polym. Sci., Part B: Polym. Phys.*, 2013, 51(7), 468.
- [9] T. Brezesinski, J. Wang, S. H. Tolbert and B. Dunn, *Nat. Mater.*, 2010, 9, 146.
- [10] U. K. Sen and S. Mitra, *Appl. Mater. Interfaces*, 2013, 5(4), 1240.
- [11] S. Y. Liew, D. A. Walsh and W. Thielemans, *RSC Adv.*, 2013, 3, 9158.
- [12] M. Ghaffari, S. Kosolwattana, Y. Zhou, N. Lachman, M. Lin, D. Bhattacharya, K. K. Gleason, B. L. Wardle and Q. M. Zhang, *Electrochim. Acta*, 2013, 112, 522.
- [13] P. Sharma and T.S. Bhatti, *Energy. Convers. Manage*, 2010, 1, 2901.
- [14] T. Lindfors, A. Österholm, J. Kauppila and M. Pesonen, *Electrochim. Acta*, 2013, 110, 428.
- [15] K. S. Ryu, Y. G. Lee, Y. S. Hong, Y. J. Park, X. L. Wu, K. M. Kim, M. G. Kang N. G. Park and S. H. Chang, *Electrochim. Acta*, 2004, 50, 843.
- [16] R. Ranjusha, K. M. Sajesh, S. Roshny, V. Lakshmi, P. Anjali, T. S. Sonia, A. S. Nair, K. R. V. Subramanian, S. V. Nair, K. P. Chennazhi and A. Balakrishnan, *Microporous Mesoporous Mater.*, 2014, 186, 30.
- [17] H. Zhou, W. Yao, G. Li, J. Wang and Y. Lu, *Carbon*, 2013, 59, 495.
- [18] Y. T. Weng and N. L. Wu, *J. Power Sources*, 2013, 238, 69.
- [19] F. Schedin, A. K. Geim, S. V. Morozov, E. W. Hill, P. Blake, M. I. Katsnelson, K. S. Novoselov, *Nat. Mater.*, 2007, 6, 652.
- [20] C. C. Hu, K. H. Chang, M. C. Lin and Y. T. Wu, *Nano Letters*, 2006, 6, 2690.
- [21] J. M. Soon and K. P. Loh, *Electrochem. Solid-State Lett.*, 2007, 10(11), 250.
- [22] M. G. Kanatzidis, R. Bissessur, D. C. DeGroot, J. L. Schindler and C. R. Kannewurf, *Chem. Mater.*, 1993, 5, 595.
- [23] R. Bissessur and W. White, *Mater. Chem. Phys.*, 2006, 99, 214.
- [24] L. Wang, J. Schindler, J. A. Thomas, C. R. Kannewurf and M. G. Kanatzidis, *Chem. Mater.*, 1995, 7, 1753.
- [25] B. Z. Lin, C. Ding, B. H. Xu, Z. J. Chen and Y. L. Chen, *Mater. Res. Bull.*, 2009, 44, 719.
- [26] A. V. Murugan, M. Quintin, M. H. Delville, G. Campet, C. S. Gopinath and K. Vijayamohanan, *J. Power Sources*, 2006, 156, 615.
- [27] M. A. Gee, R. F. Frindt, P. Joensen and S. R. Morrison, *Mater. Res. Bul.*, 1986, 21, 543.
- [28] G. Du, Z. Guo, S. Wang, R. Zeng, Z. Chen and H. Liu, *Chem. Commun.*, 2010, 46, 1106.

- [29] N. Paradee and A. Sirivat, *Polym. Int.*, 2014, 63, 106.
- [30] K. Q. Zhou, Q. J. Zhang, J. J. Liu, B. Wang, S. H. Jiang, Y. Q. Shi, Y. Hu and Z. Gui, *RSC Adv.*, 2014, 4, 13205.
- [31] J. Heising and M. G. Kanatzidis. *J. Am. Chem. Soc.*, 1999, 121, 11720.
- [32] N. Paradee and A.t Sirivat, *Polym. Int.*, 2014, 63, 106.
- [33] X. X. Bai, X. J. Hu, S. Y. Zhou, J. Yan, C. H. Sun, P. Chen and L. F. Li, *Electrochim. Acta*, 2013, 106, 219.
- [34] D. Wei, S. J. Wakeham, T. W. Ng, M. J. Thwaites, H. Brown and P. Beecher, *Electrochem. Commun.*, 2009, 11, 2285.
- [35] R. Kötz and M. Carlen, *Electrochim Acta*, 2000, 45, 2483.
- [36] Y. Q. Han, M. X. Shen, J. J. Zhu, Y. Wu and X. G. Zhang, *Polym. Compos.*, 2013, 34, 989.
- [37] K. J. Huang, L. Wang, Y. J. Liu, H. B. Wang, Y. M. Liu and L. L. Wang, *Electrochimica Acta*, 2013, 109, 587.
- [38] G. F. Ma, H. Peng, J. J. Mu, H. H. Huang, X. Z. Zhou and Z. Q. Lei, *Journal of Power Sources*, 2013, 229, 72.

Captions for Figures

Fig.1 Fig.1 FT-IR spectra of PEDOT (a), PEDOT/MoS₂ composites (b) and restacked MoS₂ (c)

Fig.2 XRD patterns of restacked MoS₂ (a) and PEDOT/MoS₂ composites (b)

Fig.3 TEM and HR-TEM images of Li-intercalated MoS₂ (a, b, c), SEM of PEDOT/ MoS₂ (d, e), EDX pattern of PEDOT/MoS₂ (f)

Fig.4 TGA curves of PEDOT and PEDOT/MoS₂ composites

Fig.5 CV curves of pure PEDOT and PEDOT/ MoS₂ composites at scan rate of 50 mV/s

Fig.6 Nyquist impedance spectra of pure PEDOT and PEDOT/ MoS₂ composites

Fig.7 Galvanostatic charge-discharge curves (a) and cycle stability (b) of electrodes with pure PEDOT and PEDOT/ MoS₂ at current density of 0.8A/g

Captions for Tables

Table 1 the data of electrical conductivities

Only for entry content:

Poly(3,4-ethylenedioxythiophene)/MoS₂ nanocomposites with enhanced electrochemical capacitance performance

Jin Wang^{*a}, Zongchao Wu^a, Huabing Yin^b, Wei Li^a, Yang Jiang^c

A facile synthesis method of PEDOT/MoS₂ nanocomposites has been developed via *in-situ* polymerization, and this work offers a strategy for preparing supercapacitors with high performance and good stability.

